

Beads Mill-Assisted Synthesis of Poly Methyl Methacrylate (PMMA)-TiO₂ Nanoparticle Composites

Mitsugi Inkyo,[†] Yusuke Tokunaga,[†] Takashi Tahara,[†] Toru Iwaki,[†] Ferry Iskandar,[‡] Christopher J. Hogan Jr.,[§] and Kikuo Okuyama^{*‡}

Kotobuki Industries Co., Ltd., 1-2-43 Hiroshiratake, Kure, Hiroshima., 737-0144, Japan, Department of Chemical Engineering, Graduate School of Engineering, Hiroshima University, 1-4-1 Kagamiyama, Higashi Hiroshima 739-8527, Japan, and Department of Energy, Environmental, & Chemical Engineering, Washington University in Saint Louis, Campus Box 1180, One Brookings Dr., Saint Louis, Missouri, 63130

A newly developed beads mill was used to create well-dispersed suspensions of TiO₂ (titania) nanoparticles in methyl methacrylate (MMA) and TiO₂-PMMA nanocomposites were synthesized by subsequent polymerization of the TiO₂-MMA suspension. Beads milling successfully broke up titania nanoparticle agglomerates with the addition of the coupling agent (3-acryloxypropyl) trimethoxysilane (APTMOs) to the titania-MMA suspension. Agglomerated particles were broken up into primary particles as small as 10 nm in suspensions with nanoparticle mass fractions as high as 0.05. Well-dispersed suspensions of titania nanoparticles had reduced UV transmission but visible light transmittance similar to pure MMA. TEM images showed that the milled nanoparticles remained well dispersed in titania-PMMA nanocomposites, and the addition of titania nanoparticles to PMMA increased the PMMA thermal stability. Spin-coated titania-PMMA films had higher refractive indices than pure PMMA films, with film of higher titania weight percent having higher refractive indices.

Introduction

Nanometer-sized particles are essential for many applications^{1–3} because nanoparticles have remarkably different electronic,⁴ optical,^{5,6} magnetic,^{7,8} and catalytic^{9,10} properties than their macroscale counterparts. It is often advantageous to incorporate nanoparticles into a matrix material, that is, a polymer solution or melt, or an elastomer, to produce a nanocomposite with additional properties brought about by the filler nanoparticles.¹¹ Recent work has shown that nanoparticle fillers within polymers can alter polymer thermomechanical properties, such as the elastic modulus,^{12,13} viscosity,¹⁴ and glass transition temperature,¹⁵ as well as optical properties.^{16,17} Advances in the preparation of nanoparticle-polymer composites will allow for the development of new types of data storage, optical, and electro-rheological materials.¹⁸ Nanoparticle-polymer composites can be prepared by either synthesizing nanoparticles within a polymer matrix^{19,20} or by dispersing nanoparticles in a monomer and polymerizing the monomer in the presence of the nanoparticles.^{21–23} The former method is limited by the fact that not all types of nanoparticles can be easily synthesized within polymer matrices. Because many nanoparticles can be synthesized in large quantities by inexpensive processes such as flame synthesis,²⁴ polymerization of a nanoparticle dispersion can be used to prepare a wider variety of nanoparticle-polymer composites than can nanoparticle production in a polymer matrix. However, the attractive force between nanoparticles in liquid suspension is often sufficiently large^{25,26} such that nanoparticles tend to agglomerate in most solvents. Poorly dispersed nanoparticles in monomer solutions will not give rise to nanoparticle-polymer nanocomposites; rather, upon polymerization they will form nanoparticle-polymer micro-

composites where large agglomerates of nanoparticles are embedded within a polymer matrix. For nanoparticle-polymer nanocomposite preparation, it is therefore necessary to develop methods to disperse nanoparticles in monomer solvents.

Mechanical milling processes are often used to break up particle agglomerates and disperse them in suspension.²⁷ Most commercial milling devices, however, are not capable of completely breaking up agglomerates of nanoparticles.²⁸ A recently developed beads mill^{28,29} was shown to be capable of breaking up supermicrometer-sized agglomerates of TiO₂ nanoparticles into 15 nm primary particles in an aqueous suspension without affecting particle crystallinity. This beads mill can operate with beads as small as 15 μm (smaller than reported for any other beads mill) because it utilizes centrifugal forces to separate beads from nanoparticle suspensions, leaving the suspensions contamination-free. The smaller beads have a lower impact energy with nanoparticles, thus preventing nanoparticle damage during the milling process while breaking up nanoparticle agglomerates.²⁸

In this study, beads milling with centrifugal bead separation was used to prepare a stable nanoparticle-monomer dispersion followed by monomer polymerization to form a nanoparticle-polymer composite material. A schematic representation of this process is shown in part a of Figure 1. To the best of our knowledge, this is the first report of the use of a milling operation for the dispersion of nanoparticles into a monomer solvent for polymer-nanoparticle composite synthesis. As a model system, TiO₂ (titania) nanoparticles were dispersed in methyl methacrylate (MMA) monomer. Poly (methyl methacrylate) (PMMA) is an important thermoplastic material that is transparent to visible light. TiO₂ nanoparticle fillers in PMMA could be used to adjust the refractive index of PMMA as well as enhance its UV light absorbing capabilities. The effects of milling time, use of coupling agents, and nanoparticle surface modification on the size distribution of titania agglomerates in MMA were determined. Dynamic light scattering, UV-vis light spectroscopy, thermogravimetric analysis, Fourier transform

* To whom correspondence should be addressed. Tel.: +81-82-424-7716. Fax.: +81-82-424-7850. E-mail: okuyama@hiroshima-u.ac.jp.

[†] Kotobuki Industries Co., Ltd.

[‡] Hiroshima University.

[§] Washington University in Saint Louis.

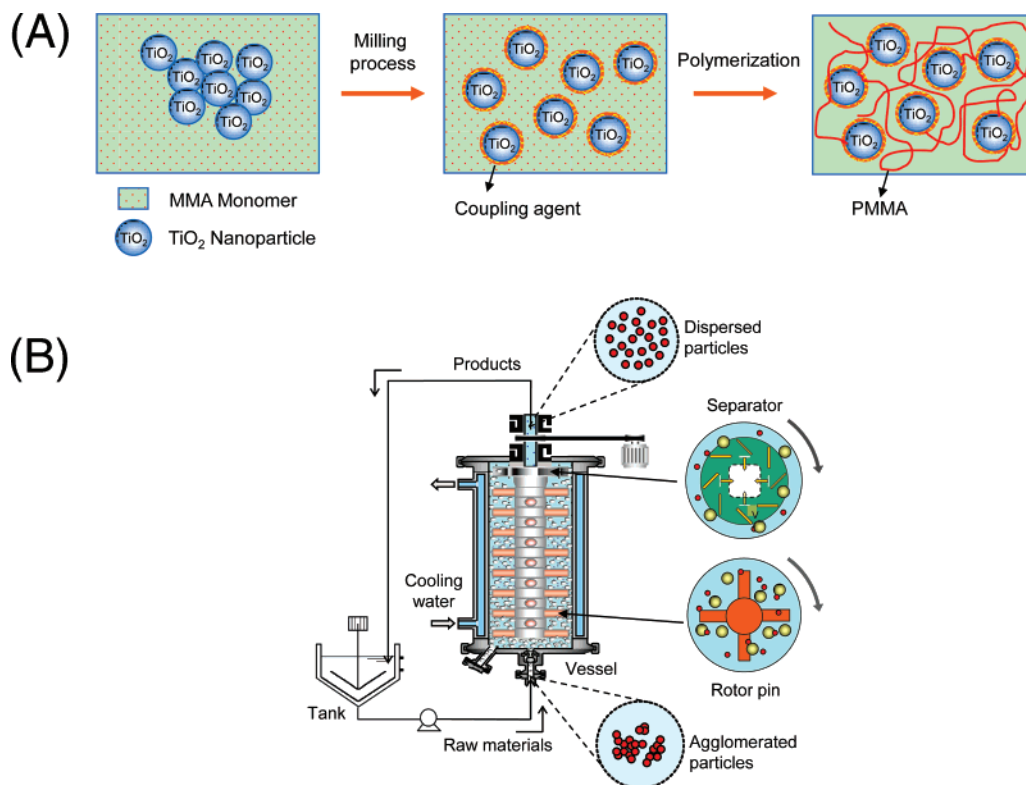


Figure 1. (a) Representation of the milling-polymerization process. (b) Schematic of the beads mill system with centrifugal bead separation.

infrared spectroscopy, and light and electron microscopy were used to evaluate the effectiveness of beads milling on the TiO₂–MMA dispersion and the properties of TiO₂–PMMA composite material.

Experimental Section

Materials. Two types of commercially produced titania nanoparticles, surface unmodified particles with a nominal primary particle size of 15 nm (MT150A, rutile phase; Tayca Co. Ltd., Japan), and alkylsilane surface-modified particles with a primary particle size of 15 nm (NKT90, anatase phase; Japan Aerosil Co. Ltd.) were used in experiments. The primary particle size of the surface-modified particles was determined by transmission electron microscopy (TEM, Japan Electron Optics Laboratory JEM-3000F, source type JEM-2010, 200 kV). The X-ray diffraction (XRD, Rigaku, RINT2550, VHF) patterns of both samples showed that they were similar phase to the manufacturer's measurements. The coupling agent (3-acryloxypropyl)trimethoxysilane (APTMO; KBM5103, Shinetsu Co. Ltd., Japan) was also used in nanoparticle suspensions. The beads mill contained 15 μm ZrO₂ (zirconia) beads (Neturen Co., Ltd. Tokyo, Japan). Prior to the preparation of nanoparticle suspensions, the MMA monomer solvent (Mitsubishi Gas Chemical, 99.8% purity, 0.569 cp at 25 °C) was purified by distillation. Azobisisobutyronitrile (AIBN, Otsuka Chemical Co., Ltd. purity: >99%) was used as a polymerization initiator.

Milling Process. A schematic of the beads mill is shown in part b of Figure 1 and a detailed description of the beads mill is found elsewhere.^{28,29} The beads mill is composed of an 80 mL vessel, a pump, and a mixing tank. Nanoparticle suspensions are pumped into the vessel, which contains the zirconia beads and a centrifugation rotor. Beads are agitated in the lower portion of the vessel (the dispersing section), which drives the break-up of agglomerated particles. The suspension is pumped from the dispersing section to the upper region (the centrifugation

section) where centrifugal force is used to separate the zirconia beads from the nanoparticle suspension. The centrifugal force can also remove large nanoparticle aggregates until they are broken into primary particles. The nanoparticle suspension is then recycled back to the dispersing section. To prevent temperature increases in the system, the vessel is housed in a cooling water jacket and is completely sealed from the outside environment.

For the break-up of titania agglomerates suspended in MMA, titania–MMA suspensions with mass fractions of titania ranging from 0.01 to 0.1 were pumped through the beads mill with a recirculating mass flowrate of 10 kg/h (29 s residence time in the milling region, 25 cycles per hour, 144 s total recirculation time). Nanoparticle suspensions were prepared with and without the addition of a coupling agent. Centrifugal forces for bead separation in the upper part of the vessel were generated by rotating the outer cylindrical wall at a speed of 10 m/s. The zirconia beads occupied 65% of the vessel volume.

Polymerization. After milling, the titania–MMA suspension was transferred to a reaction flask, to which the polymerization initiator AIBN was added such that there was an AIBN to MMA mass ratio of 0.001. Polymerization was carried out at 60 °C in an N₂ atmosphere for 6 h.

Film Preparation. Titania–PMMA nanocomposite (1 g) was dissolved in 20 mL of tetrahydrofuran in a glass flask (50 mL) and spin-coated using a spin coater (1H-D7, Mikasa) onto sapphire substrates (Kyocera Co., Ltd). Spin coating was performed with a dropping volume of 1 mL at 2000 rpm.

Material Characterization. Particle-size distributions after selected milling times were measured using dynamic light scattering (DLS) with an FPAR-1000 (Otsuka Denshi. Co., plastic cuvettes, 1 mL volume). Size-distribution measurements were made without dilution in duplicate to ensure reproducibility. The refractive index and viscosity of MMA were used as input parameters for an instrument built-in software package

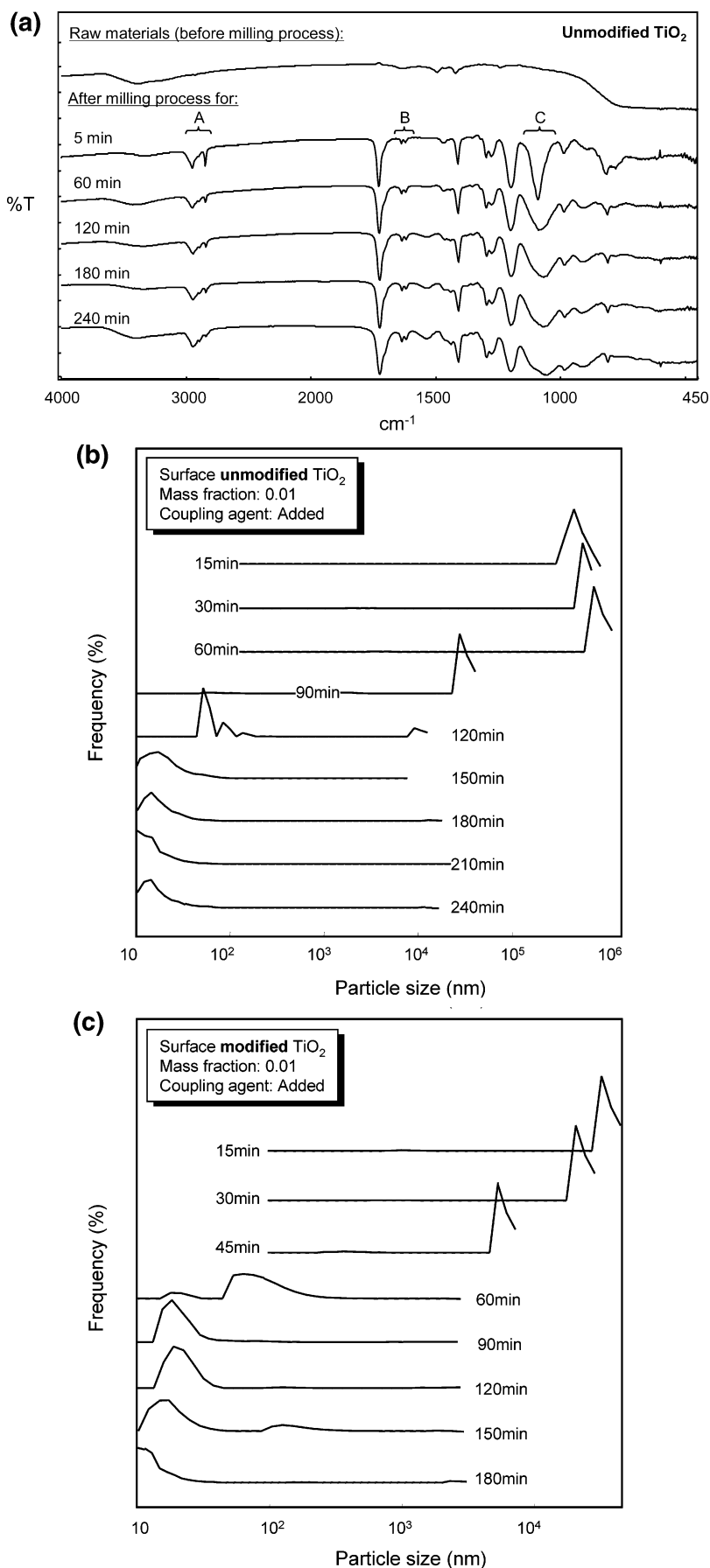


Figure 2. (a) FTIR spectra of titania particles and titania–MMA suspensions with APTMOS after selected milling times (A, C–H stretching in methoxy functional groups; B, C=C in APTMOS; C, Si–O stretching in Si–O–R groups). (b) Particle-size distributions of unmodified and (c) surface-modified TiO₂ particles in MMA after selected milling times with the addition of a coupling agent. The titania mass fraction in the suspensions was 0.01 in both (b) and (c).

for size-distribution deconvolution. The samples were dried and mixed with KBr powder for FTIR measurement (PerkinElmer, Spectrum One System A, range: $\sim 7800\text{--}350\text{ cm}^{-1}$, resolution: $\sim 0.5\text{--}64\text{ cm}^{-1}$, transmission mode). The samples were poured in a quartz cell of 1 cm optical depth and measured by UV-vis spectroscopy (U-2810, Hitachi, 190-1100 nm). TiO₂ nanoparticles after MMA polymerization were observed using transmission electron microscopy. To obtain TEM images (JEOL-JEM-2010, 200kV), the TiO₂-PMMA composite was cut into thin layers using a microtome, and a single, thin layer was placed on a TEM grid. The thermal properties of TiO₂-PMMA nanocomposites were measured with a thermogravimetric analyzer (Shimadzu Thermo Plus TG8120; maximum temperature, 800 °C; temperature ramp rate, 5 °C/min in N₂). A prism coupler (Model 2010, Metricon Corp.) was used to measure the refractive index of spin-coated composite films at a wavelength of 633 nm.

Results and Discussion

TiO₂ Agglomerate Break-up in MMA. To prepare well-dispersed nanoparticle suspensions, it is necessary to optimize both the milling operating conditions as well as control the attractive and repulsive forces between nanoparticles and nanoparticle agglomerates. As agglomerates are broken up, the number concentration of particles in the suspension substantially increases, which can lead to reagglomeration of particles, particularly if there is an attractive force between particles.³⁰ Surface modification of nanoparticles prior to suspension preparation may prevent reagglomeration from occurring. The performance of the beads mill in breaking nanoparticle agglomerates of both unmodified and surface-modified titania nanoparticles suspended in MMA without any coupling agents in the suspension was first investigated. It was found that surface modification of the nanoparticles had no effect on the beads mill performance. Initially, the titania nanoparticles were agglomerated with agglomerate sizes in the supermicrometer size range. DLS measurements showed that large agglomerates remained in the suspension throughout the milling process. The chemical composition of the suspension was checked after milling by inductively couple plasma spectroscopy,²⁸ and it was found that the zirconia beads did not contaminate the sample (they were separated from the suspension by centrifugation in the mill, as they are denser than titania), and the large agglomerates were in fact titania. Therefore, beads milling had little to no effect on the particle-size distribution, and, presumably, any agglomerates broken during the milling process reagglomerated rapidly. Agglomerated titania nanoparticles also settled out of suspension from the MMA monomer after several hours post milling.

The inability of the beads mill to disperse both unmodified and surface-modified titania nanoparticles implies that the TiO₂ were strongly attracted to each other (large Hamaker constant) in MMA. Silane coupling agents are typically used to bond inorganic materials to organic materials;²¹ thus, trace amounts (2 g of coupling agent per square meter of titania primary particle surface area for all experiments hereafter) of the coupling agent APTMOS were added to the titania-MMA suspension prior to milling. FTIR spectra of pure titania powder as well as the unmodified TiO₂-MMA suspension with APTMOS after beads milling times of 5, 60, 120, 180, and 240 min are shown in part a of Figure 2. In the suspension FTIR spectra, peaks at 2840 cm⁻¹ (A, C-H stretching in methoxy functional groups), 1640-1590 cm⁻¹ (B, C=C in APTMOS), and 1110-1000 cm⁻¹ (C, Si-O stretching in Si-O-R groups)

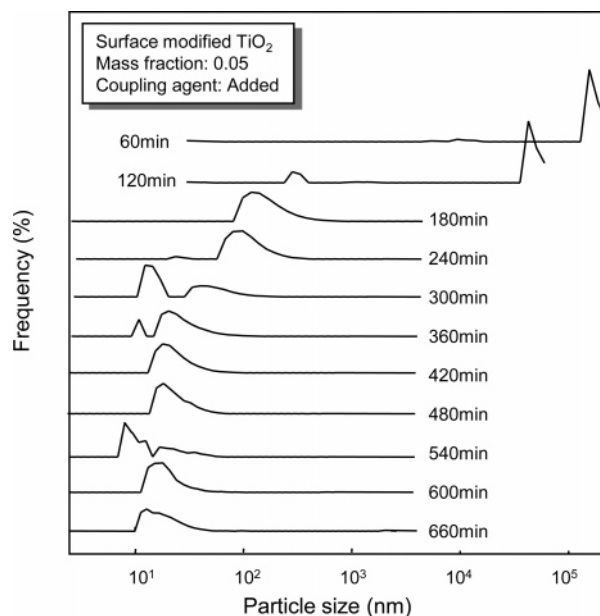


Figure 3. Particle-size distributions of the surface-modified TiO₂ particles in MMA after selected milling times with the addition of a coupling agent. The titania mass fraction in the suspensions was 0.05.

were apparent. With increasing milling time, the peak at 1110-1000 cm⁻¹ decreased in intensity due to substitution of a methyl group with titanium in Si-O-R bonds. FTIR spectra therefore show that the coupling agent coated the titania particles during the milling process. With the addition of the coupling agent, beads milling was able to successfully break up nanoparticle agglomerates into particles with sizes on the order of the primary particles. The size distributions of MMA suspensions of unmodified and surface-modified titania nanoparticles with titania mass fraction of 0.01 are shown in parts b and c of Figure 2, respectively (y axis, intensity from DLS measurements). Initially, the exposed surfaces of titania agglomerates were coated with the coupling agent. As beads milling proceeded, new titania surfaces were exposed, which, in turn, were coated by the coupling agent, preventing reagglomeration from occurring. The time required to break agglomerates into sizes close to the primary particle sizes was longer for the unmodified titania (150 min) as compared to the surface-modified titania (90 min). This was presumably due to the fact that the agglomerates of unmodified titania nanoparticles had stronger interparticle forces holding them together than did the surface-modified titania particles. Collisions between beads and agglomerates would have had energies that were functions of bead and agglomerate velocity, bead size, and agglomerate size,^{28,31} but would have been relatively independent of the interparticle forces holding the agglomerate together. Only a certain fraction of collisions would have had sufficient energy to disrupt interparticle forces within an agglomerate. The energy distribution of agglomerate-bead collisions was likely the same for unmodified and surface-modified titania. The interparticle forces between unmodified titania particles were, however, presumably stronger than the forces between surface-modified titania particles. A smaller fraction of collisions then resulted in agglomerate breakage; thus, a longer milling time was needed to break agglomerates of unmodified titania nanoparticles. Reducing the necessary milling time, therefore, cannot only be accomplished by optimizing beads milling conditions²⁸ but also by using nanoparticles, which only form weakly bonded, or soft, agglomerates.³²

(a) Milling time (min):

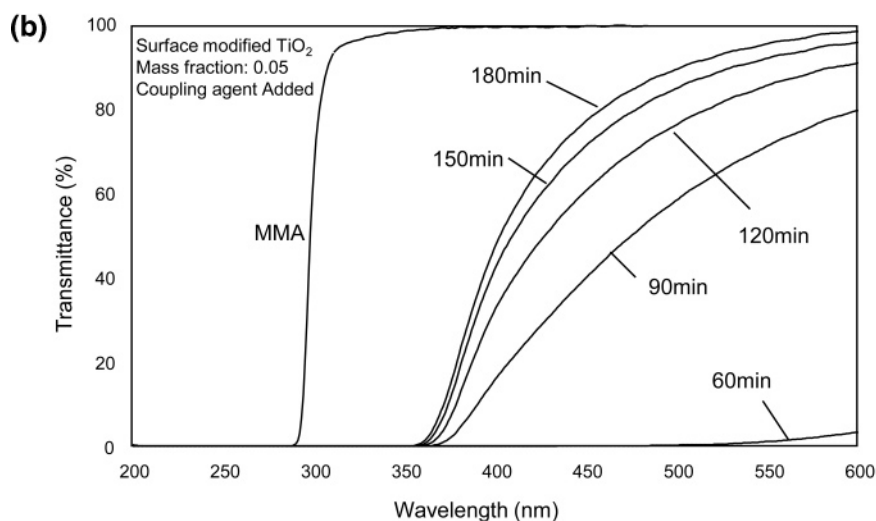
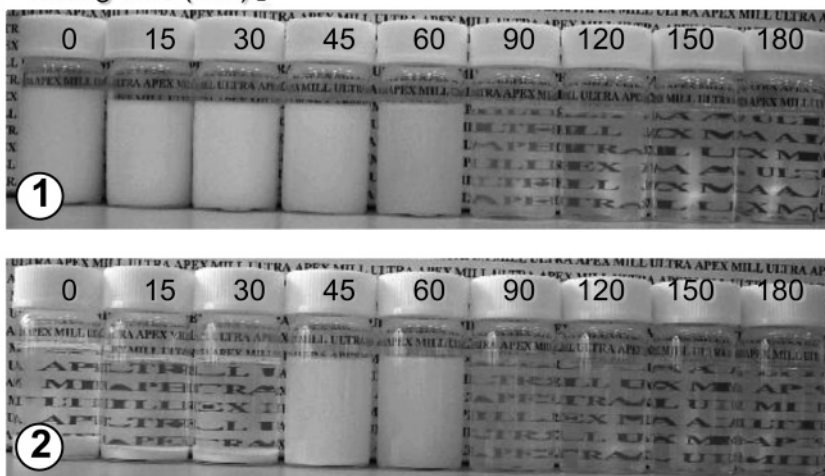


Figure 4. (a) Images of surface-modified titania particles in MMA with a coupling agent added examined immediately after milling (1a) and 24 h after milling (2). From left to right, the milling time for each of the sample vials shown was 0, 15, 30, 45, 60, 90, 120, 150, and 180 min, respectively. (b) UV-vis transmittance spectra of surface-modified titania particles in MMA with a coupling agent added after selected milling times.

Figure 3 shows the size distributions of MMA suspensions of surface-modified titania with a titania mass fraction of 0.05 and a coupling agent added to the suspension. Increasing the concentration of nanoparticles in the suspension 5 times increased the rate of agglomeration roughly by a factor of 25^{33} and led to the formation of larger agglomerates in the suspension ($>100 \mu\text{m}$). The milling time necessary to break up agglomerates was several times longer than was necessary for a suspension with a titania mass fraction of 0.01. At a high particle number concentration, the rate of reagglomeration is sufficiently high for particles to reaggregate back to their unmilled size while being recycled through the beads mill, that is, at a high number concentration the rate of reagglomeration can be greater than the rate of agglomerate break-up.³¹ The particle number concentration at which reagglomeration begins to occur is a function of the attractive and repulsive forces between particles and agglomerates as well as the particle and agglomerate sizes and polydispersity.³³ Here, the addition of a coupling agent to suspensions served to decrease the strength of the attractive forces between particles and agglomerates in suspension, and, although a longer milling time was needed, the beads mill was able to successfully break up titania agglomerates into primary particles in suspensions with a mass fraction of 0.05.

Visual analysis of suspensions provided further evidence of the degree to which agglomerates were dispersed by beads milling. Part a of Figure 4 shows samples of surface-modified titania nanoparticles (with coupling agent added, titania mass fraction of 0.01) after selected beads milling times (top row, 1) and after selected beads milling times and 24 h in the sample vial (bottom row, 2). After short milling times (less than 60 min), the samples were opaque immediately after milling and agglomerated nanoparticles settled to the bottom of the sample vials after 24 h. For longer milling times, the suspension consisted of primary titania nanoparticles and nanosized agglomerates; thus, suspensions were clear (the and a slight tint of the suspensions was due to bonding of the coupling agent with the nanoparticles). Because reagglomeration was prevented by the coupling agent, particles remained nanosized and did not settle out of the suspension after 24 h.

The UV-vis transmittance spectra of surface-modified milled titania suspensions, a titania mass fraction of 0.01, and coupling agent added are shown in part b of Figure 4. The transmittance spectrum of MMA monomer is also shown. MMA monomer, like PMMA, has almost 100% transmittance at wavelengths greater than 300 nm. As expected based on size-distribution measurements, the transmittance of titania-MMA suspensions at wavelengths greater than 350 nm increased with increasing

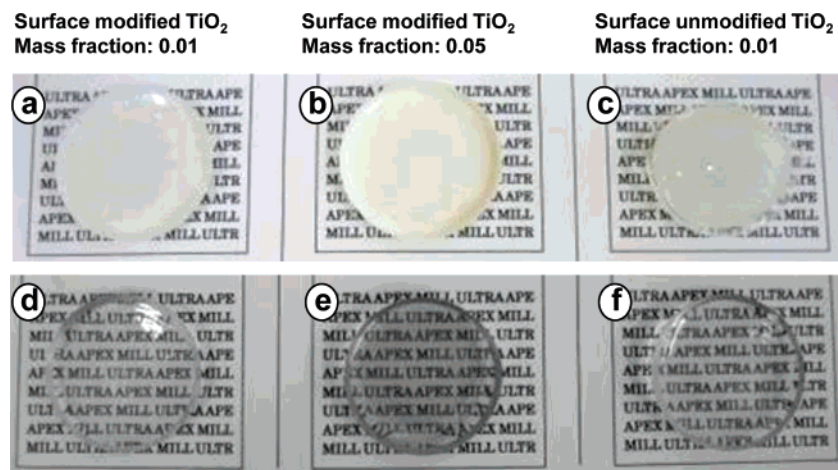


Figure 5. Images of titania-PMMA composites made from the polymerization of (a-c) unground and (d-f) milled titania-MMA suspensions.

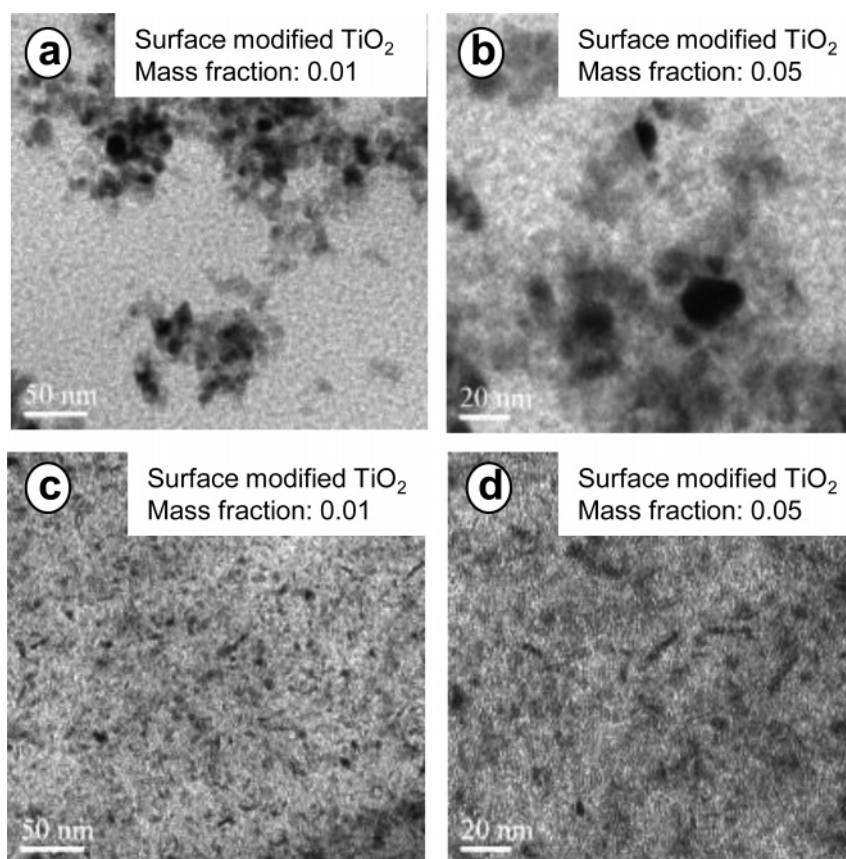


Figure 6. TEM images of titania particles in titania-PMMA composites made from the polymerization of (a-b) unground and (c-d) milled titania-MMA suspensions.

milling time because the amount of light scattering decreased as agglomerates were dispersed into primary particles. In the 300–350 nm UV range, however, the suspensions were almost completely absorbing, regardless of the amount of milling time. Therefore, well-dispersed titania nanoparticles could be used to enhance the UV light absorbing properties of PMMA while still allowing the transmittance of visible light. After a period of 30 days, the suspensions were found to have the same transmittance spectra, showing that well-dispersed titania suspensions were very stable.

Titania-PMMA Nanocomposites. Digital images of titania-PMMA nanocomposites formed by the polymerization of a titania-MMA suspension are shown in Figure 5. The titania-PMMA composites shown in parts a-c of Figure 5 were formed from the polymerization of surface-modified titania-MMA

suspensions with the addition of the coupling agent where no beads milling was used (titania and MMA were instead ground with a mortar and pestle and mixed with MMA), whereas the titania-PMMA composites shown in parts d-f of Figure 5 were formed from the polymerization of surface-modified titania-MMA suspensions with the addition of the coupling agent that had been processed in the beads mill. The titania mass fractions were 0.01, 0.05, and 0.01 for parts a and d of Figure 5, parts b and e of Figure 5, and parts c and f of Figure 5, respectively. The milling times for parts d, e, and f of Figure 5 were 180, 660, and 240 min, respectively. Like the monomer suspensions, the titania-PMMA composites synthesized from unground suspensions were opaque, whereas the composites synthesized from milled suspensions transmitted visible light. TEM images of surface-modified titania-PMMA composites synthesized

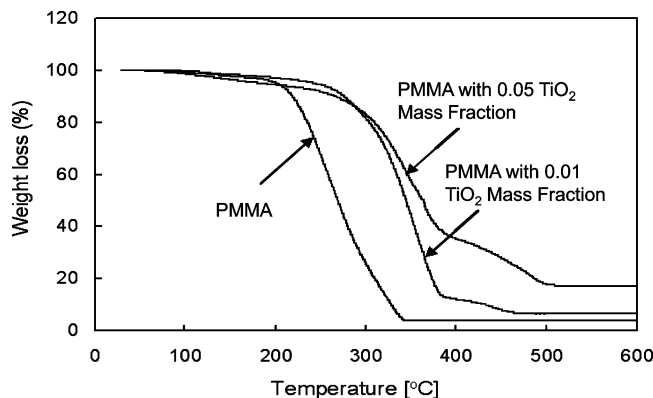


Figure 7. Weight loss vs temperature curves of synthesized TiO₂–PMMA nanocomposite samples and pure PMMA. The heating rate was 5 °C/min.

from unmilled titania–MMA suspensions (a,b) and (c,d) milled titania–MMA suspensions for 660 min are shown in Figure 7 (both with the addition of the coupling agent). The mass fraction of titania in suspension was 0.01 for parts a and c of Figure 6 and 0.05 for parts b and d of Figure 6. The TEM images agree well with the size distributions of titania particles measured by dynamic light scattering in the MMA suspension. Unmilled particles were highly agglomerated, whereas milled particles were well dispersed, allowing for the synthesis of titania–PMMA nanocomposites. The weight-loss versus temperature curves for PMMA and PMMA–TiO₂ nanocomposites (titania–MMA suspension milled for 240 min) with 0.01 and 0.05 TiO₂ mass fractions are shown in Figure 7. Typically, PMMA thermally degrades in two steps.³⁴ The polymer will first decompose into smaller polymer segments, and, subsequently, each segment will further decompose into monomers. Thermogravimetric analysis therefore could only be used to examine the second step of this process, as minimal weight loss occurs in the first step. The addition of titania nanoparticles to PMMA to create PMMA–TiO₂ nanocomposites increased the temperature at which weight loss occurred, showing that PMMA–TiO₂ nanocomposites are more thermally stable than PMMA alone. The degradation temperature did not increase significantly as the titania mass fraction was increased from 0.01 to 0.05. This result may be dependent on the molecular weight of the PMMA and the size of the TiO₂ nanoparticles. The increase in decomposition temperature was due to the interfacial interaction between titania and PMMA, and the amount of the surface contact between PMMA and TiO₂ would be dependent on both the molecular weight of the PMMA and the TiO₂ nanoparticle size. The refractive indices of titania–PMMA nanocomposite films are shown in Figure 8 as a function of titania weight percent. The refractive index of samples at 633 nm were 1.4853, 1.4898, 1.4958, and 1.5070 for pure PMMA, 0.02, 0.05, and 0.10 TiO₂ mass fraction in PMMA films, respectively. The increase in refractive index can be predicted using Drude's model, given as,

$$n^2 - 1 = V_a(n_a^2 - 1) + V_b(n_b^2 - 1) \quad (1)$$

where n , n_a , and n_b are the refractive indexes of composite polymer, PMMA, and TiO₂ ($n_b = 2.76$), respectively, and V_a and V_b are the volume fractions of PMMA and TiO₂, respectively. Measured refractive indices were slightly lower than was predicted by the model, which may be due to the presence of impurities in the titania particles or the addition of coupling agents during beads milling.

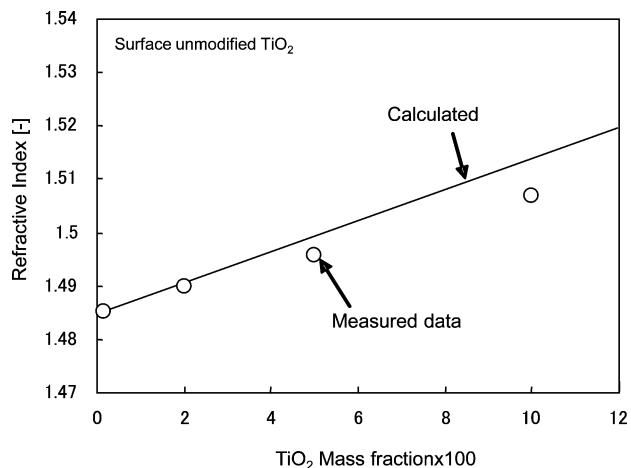


Figure 8. Composite film refractive index as a function of titania mass fraction.

Conclusions

A new type of beads mill was used to process suspensions of titania and MMA to break up titania nanoparticle agglomerates. Without the addition of a silane coupling agent, particle reagglomeration was rapid enough such that any agglomerates broken up by beads milling reagglomerated as the particles recirculated through the beads mill. With the addition of a silane coupling agent, the beads mill was capable of breaking up nanoparticle agglomerates in suspensions where the nanoparticle mass fraction was as high as 0.05. Well-dispersed titania nanoparticles have little effect on the transmittance of visible light through MMA but enhance the UV absorbing properties of MMA. By polymerizing MMA in titania–MMA suspensions, titania–PMMA nanocomposites were formed. PMMA in PMMA–titania nanocomposites was more thermally stable than PMMA alone. The results of these experiments show that beads milling with a newly developed beads mill is a robust and simple technique for dispersing nanoparticles into organic solvents, which is one of the major obstacles to overcome in polymer–nanoparticle composite synthesis.

Acknowledgment

We thank to Prof. Dr. Takeshi Shiono (Hiroshima University) for helpful discussions. C.J.H. acknowledges support from an NSF graduate research fellowship.

Literature Cited

- (1) Schmid, G.; Talapin, D. V.; Shevchenko, E. V. In *Nanoparticles: From Theory to Applications*, Schmid, G., Ed.; VCH: Weinheim, Germany, 2004; p 251.
- (2) Haes, A. J.; Van Duyne, R. P. *J. Am. Chem. Soc.* **2002**, *124*, 10596.
- (3) Alivisatos, A. P. *Science* **1996**, *271*, 933.
- (4) Chen, S. W.; Murray, R. W.; Feldberg, S. W. *J. Phys. Chem. B* **1998**, *102*, 9898.
- (5) Templeton, A. C.; Pietron, J. J.; Murray, R. W.; Mulvaney, P. J. *Phys. Chem. B* **2000**, *104*, 564.
- (6) Jin, R. C.; Cao, Y. W.; Mirkin, C. A.; Kelly, K. L.; Schatz, G. C.; Zheng, J. G. *Science* **2001**, *294*, 1901.
- (7) Park, J. I.; Cheon, J. *J. Am. Chem. Soc.* **2001**, *123*, 5743.
- (8) Shevchenko, E. V.; Talapin, D. V.; Schnablegger, H.; Kornowski, A.; Festin, O.; Svedlindh, P.; Haase, M.; Weller, H. *J. Am. Chem. Soc.* **2003**, *125*, 9090.
- (9) Li, Y.; Boone, E.; El-Sayed, M. A. *Langmuir* **2002**, *18*, 4921.
- (10) Tsunoyama, H.; Sakurai, H.; Ichikuni, N.; Negishi, Y.; Tsukuda, T. *Langmuir* **2004**, *20*, 11293.
- (11) Oberdisse, J. *Soft Matter* **2006**, *2*, 29.
- (12) Zhao, H. X.; Li, R. K. Y. *J. Polym. Sci., Part B: Polym. Phys.* **2005**, *43*, 3652.

- (13) Kuo, M. C.; Tsai, C. M.; Huang, J. C.; Chen, M. *Mater. Chem. Phys.* **2005**, *90*, 185.
- (14) Cole, D. H.; Shull, K. R.; Baldo, P.; Rehn, L. *Macromolecules* **1999**, *32*, 771.
- (15) Ash, B. J.; Siegel, R. W.; Schadler, L. S. *J. Polym. Sci., Part B: Polym. Phys.* **2004**, *42*, 4371.
- (16) Carter, S. A.; Scott, J. C.; Brock, P. J. *Appl. Phys. Lett.* **1997**, *71*, 1145.
- (17) Benaissa, M.; JoseYacaman, M.; Xiao, T. D.; Strutt, P. R. *Appl. Phys. Lett.* **1997**, *71*, 3685.
- (18) Schmidt, G.; Malwitz, M. M. *Curr. Opin. Colloid Interface Sci.* **2003**, *8*, 103.
- (19) Pramanik, P. *Bull. Mater. Sci.* **1995**, *18*, 819.
- (20) Sambhy, V.; MacBride, M. M.; Peterson, B. R.; Sen, A. *J. Am. Chem. Soc.* **2006**, *128*, 9798.
- (21) Yang, M. J.; Dan, Y. *J. Appl. Polym. Sci.* **2006**, *101*, 4056.
- (22) Pavel, F. M.; Mackay, R. A. *Langmuir* **2000**, *16*, 8568.
- (23) Raula, J.; Shan, J.; Nuopponen, M.; Niskanen, A.; Jiang, H.; Kauppinen, E. I.; Tenhu, H. *Langmuir* **2003**, *19*, 3499.
- (24) Kammler, H. K.; Madler, L.; Pratsinis, S. E. *Chem. Eng. Technol.* **2001**, *24*, 583.
- (25) Artelt, C.; Schmid, H. J.; Peukert, W. *J. Aerosol Sci.* **2005**, *36*, 147.
- (26) Israelachvili, J. *Intermolecular and Surface Forces*; Academic Press: London, 2000.
- (27) Muller, F.; Peukert, W.; Polke, R.; Stenger, F. *Int. J. Miner. Process.* **2004**, *74*, S31.
- (28) Inkyo, M.; Tahara, T.; Iwaki, T.; Iskandar, F.; Hogan, C. J.; Okuyama, K. *J. Colloids Interface Sci.* **2006**, *304*, 535.
- (29) Inkyo, M.; Tahara, T. *J. Soc. Powder Technol., Japan* **2004**, *41*, 578.
- (30) Sommer, M.; Stenger, F.; Peukert, W.; Wagner, N. J. *Chem. Eng. Sci.* **2006**, *61*, 135.
- (31) Stenger, F.; Mende, S.; Schwedes, J.; Peukert, W. *Chem. Eng. Sci.* **2005**, *60*, 4557.
- (32) Tsantilis, S.; Pratsinis, S. E. *Langmuir* **2004**, *20*, 5933.
- (33) Friedlander, S. K., *Smoke, Dust, and Haze: Fundamentals of Aerosol Dynamics*, 2nd ed.; Oxford University Press: New York, Oxford, 2000.
- (34) Yang, F.; Nelson, G. L. *J. Appl. Polym. Sci.* **2004**, *91*, 3844.

Received for review August 6, 2007

Revised manuscript received February 1, 2008

Accepted February 8, 2008

IE071069J